Biosensors

DOI: 10.1002/anie.201205687

Continuous Stochastic Detection of Amino Acid Enantiomers with a Protein Nanopore**

*Arnold J. Boersma and Hagan Bayley**

Amino acids are critical to life; they are the building blocks of proteins and key structural elements in many pharmaceuticals. Enantiomeric purity is crucial for amino acid function, and hence *ee* determination has been intensively studied. Routine *ee* determination still relies on derivatization of the amino acid before analysis with one of a range of chiral HPLC columns.[1] However, derivatization might influence the *ee*, and it hinders rapid screening. The *ee* of underivatized amino acids can also be determined by chiral column chromatography,[1] NMR spectroscopy with chiral shift reagents,[2] and mass spectrometry in combination with chiral hosts.[3] More recent techniques for the *ee* determination of underivatized amino acids rely on monitoring affinity differences towards chiral receptors with various optical techniques.[4–6]

Here, we show that the *ee* of underivatized amino acids can be monitored by using a modified protein nanopore, α-hemolysin (αHL), as a stochastic sensor. In stochastic detection, the ionic current flowing through a single nanopore is modulated when an analyte binds at an engineered site within the pore lumen. The frequency of occurrence of the binding events reveals the concentration of an analyte, while the nature of the events (e.g. amplitude of block and mean duration of block) yields the identity of the analyte. By using engineered sites that are only partly selective, several different analytes can be examined with the same pore because only one analyte is bound at a time.[7]

An especially successful approach for the stochastic detection of organic molecules has been the use of β-cyclodextrin and other adapters. The adapters lodge non-covalently within the nanopore, and bind analytes through host–guest interactions.[8] The chiral environment of the cyclodextrin has been exploited for chiral discrimination of the small drug molecules ibuprofen and thalidomide.[9] This approach relies on the formation of a diastereomeric complex between the chiral drug molecule and the cyclodextrin, which results in slightly different current block levels for the enantiomers. Later, cyclodextrin lodged in a glass pipette was employed for stochastic detection of ibuprofen and catechin.[10] Multiple cyclodextrins have also been attached covalently inside a conical pore in polyethylene terephthalate (PET), and were used for the selective binding of L-histidine over D-histidine.[11] The latter method lacks the advantages of stochastic sensing because single binding events are not observed. Further, we found that β-cyclodextrin is not suitable for stochastic sensing of amino acids with protein nanopores: no detectable tyrosine binding was observed (see the Supporting Information), which is most likely due to the low affinity of amino acids for cyclodextrin.[12]

Previously, we observed that neurotransmitters including the amino acid glutamate can bind within a protein nanopore

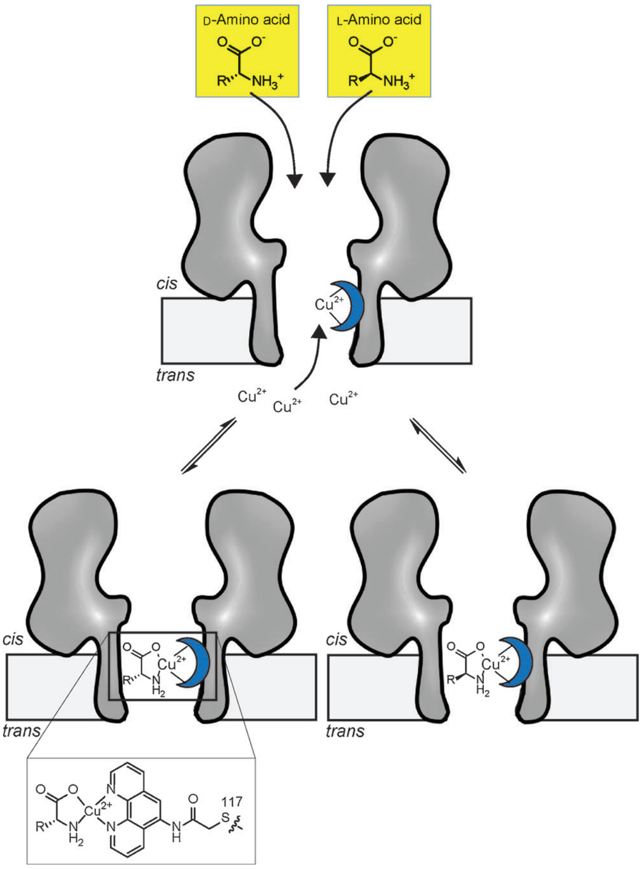

Figure 1. Stochastic detection of the enantiomers of an amino acid by using a Cu^{II}–phenanthroline protein nanopore. The α-hemolysin nanopore is modified covalently at Cys-117 on one subunit with an iodoacetamide-containing phenanthroline (see the Supporting Information). Copper(II) is added from the *trans* compartment, and binds strongly to the phenanthroline-modified pore. D- and L-amino acids are added from the *cis* compartment and reversibly bind to the copper ion within the pore. The presence of the amino acid leads to a transient decrease in the conductance of the pore, the extent of which depends on which enantiomer is bound.

---

[*] Dr. A. J. Boersma, Prof. Dr. H. Bayley
Department of Chemistry, University of Oxford
Oxford OX1 3TA (UK)
E-mail: hagan.bayley@chem.ox.ac.uk

[**] This work was supported by the Netherlands Organization for Scientific Research (NWO, Rubicon Fellowship, A.J.B.), the Medical Research Council, and Oxford Nanopore Technologies.

Supporting information for this article is available on the WWW under http://dx.doi.org/10.1002/anie.201205687.

by making use of metal coordination.[13] In this approach, a phenanthroline ring is installed within the β barrel of the pore by site-specific chemical modification of one of the seven subunits of the pore. The phenanthroline coordinates a copper(II) ion presented from the *trans* side of the bilayer. Amino acids added from the *cis* side coordinate the copper(II) through their amine nitrogen and a carboxylic acid oxygen.[14–16] The coordination of an individual amino acid results in an ionic current block. We reasoned that the interaction of amino acids with the chiral environment provided by the αHL pore might result in a different current block for each enantiomer. The time-dependent generation of an *ee* would then be determined by counting the events generated by each enantiomer (Figure 1).

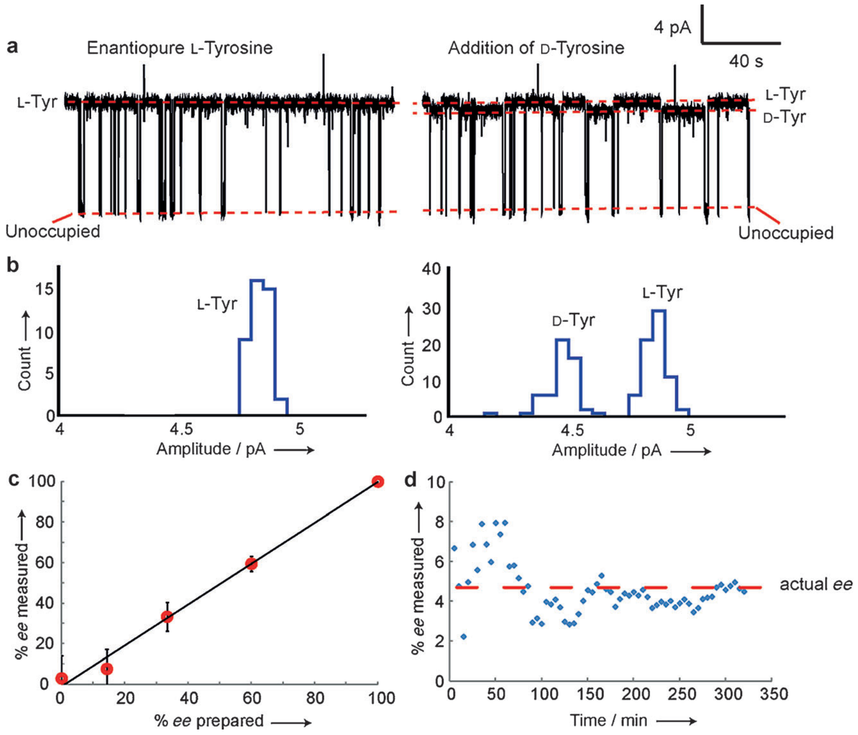

Figure 2. Binding characteristics of D- and L-tyrosine to the Cu^{II}–phenanthroline protein nanopore. a) Current trace with 3 μM L-tyrosine in the *cis* compartment (left). 3 μM D-tyrosine was subsequently added to the same compartment (right). Conditions: −50 mV, 10 μM CuCl_2 added from the *trans* compartment, 1.0 M KCl, 10 mM 3-(*N*-morpholino)propanesulfonic acid (MOPS), pH 7.0. b) Event histograms showing the distributions of the amplitudes of the current blocks induced by L-tyrosine (left) and by D- and L-tyrosine (right). c) Relationship between the *ee* in known mixtures of D- and L-tyrosine and the *ee* determined with the Cu^{II}–phenanthroline protein nanopore. Calibration curves were created by titrating D-tyrosine in 2.5 μM increments into a 10 μM L-tyrosine solution. The *ee* was determined after recording for 10 minutes by counting the events corresponding to each enantiomer. The slope is 1.0 ± 0.1, with $R^2 = 0.990 \pm 0.003$ ($n = 3$ pores), which is in accord with the similar association rate constants determined for D- and L-tyrosine. Therefore, subsequently, the readout was taken as the *ee* of the mixture. d) Relationship between the determined *ee* and the measurement time. The *ee* of tyrosine was determined every 5 minutes with the data accumulated at that point. The concentration of L-tyrosine was 5.88 μM, the concentration of D-tyrosine was 6.46 μM, corresponding to an *ee* of 4.69 %.

First, the ability of the Cu^{II}-phenanthroline pore to discriminate between the enantiomers of tyrosine was tested. Tyrosine has a high affinity for copper(II), and the aromatic ring is believed to interact with the copper(II) through a cation–π interaction.[17,18] The addition of 3 μM L-tyrosine to the *cis* compartment at −50 mV resulted in reversible current blocks with an average lifetime of 11 ± 2 s ($n = 3$ pores; Figure 2a), an association rate constant of $(8.3 \pm 0.7) \times 10^4\,\text{M}^{-1}\text{s}^{-1}$, and a dissociation rate constant of $(9 \pm 1) \times 10^{-2}\,\text{s}^{-1}$. The current block by L-tyrosine was 4.9 ± 0.1 pA ($n = 43$ events). Current blocks were not observed with the wild-type αHL pore. The subsequent addition of 3 μM D-tyrosine produced additional binding events with a different extent of block of 4.5 ± 0.1 pA ($n = 53$ events), a difference of 0.4 ± 0.1 pA (Figure 2ab). The difference in current block between the enantiomers was about 1 % of the total current (−39 ± 1 pA at −50 mV, $n = 7$ pores), independent of the applied potential (see the Supporting Information) and showed a baseline separation in current event histograms (Figure 2b). The kinetic parameters for D-tyrosine binding were similar to those of L-tyrosine: association rate constant of $(8.6 \pm 0.8) \times 10^4\,\text{M}^{-1}\text{s}^{-1}$; dissociation rate constant of $(11 \pm 1) \times 10^{-2}\,\text{s}^{-1}$.

To obtain a quantitative estimate of *ee*, a calibration curve was produced by counting binding events arising from known mixtures of D- and L-tyrosine (Figure 2c). The slope of 1.0 ± 0.1 is consistent with the observation that the association rate constants of the enantiomers are similar. Hence, calibration is not required for *ee* determination. The accuracy of the *ee* determination increases with time, as more events are recorded (Figure 2d). For tyrosine, the *ee* determined after 5 minutes is a rough estimate, while extension of the measurement time gives errors of < 0.5 % *ee* compared to the actual *ee*. Tyrosine has one of the longest average dwell times of the amino acids tested; shorter dwell times and more rapid binding would lead to greater accuracy over a fixed recording period, because more events would be registered. These alterations in kinetics might be promoted by modification of the protein or the phenanthroline ligand.

The approach is also applicable to other amino acids. Besides tyrosine, the enantiomers of phenylalanine, cysteine, and aspartic acid (Figure 3a) were distinguished on the basis of their current block amplitudes. In each of these cases, the D enantiomer gave a larger current block compared to the L enantiomer, which is opposite to the case of tyrosine in which the L enantiomer gave the larger block. Interestingly, the tryptophan enantiomers could be distinguished by the noise during the current block, which is quantified by the root-mean-square (rms) current noise. The current block corresponding to L-tryptophan had a higher rms current noise

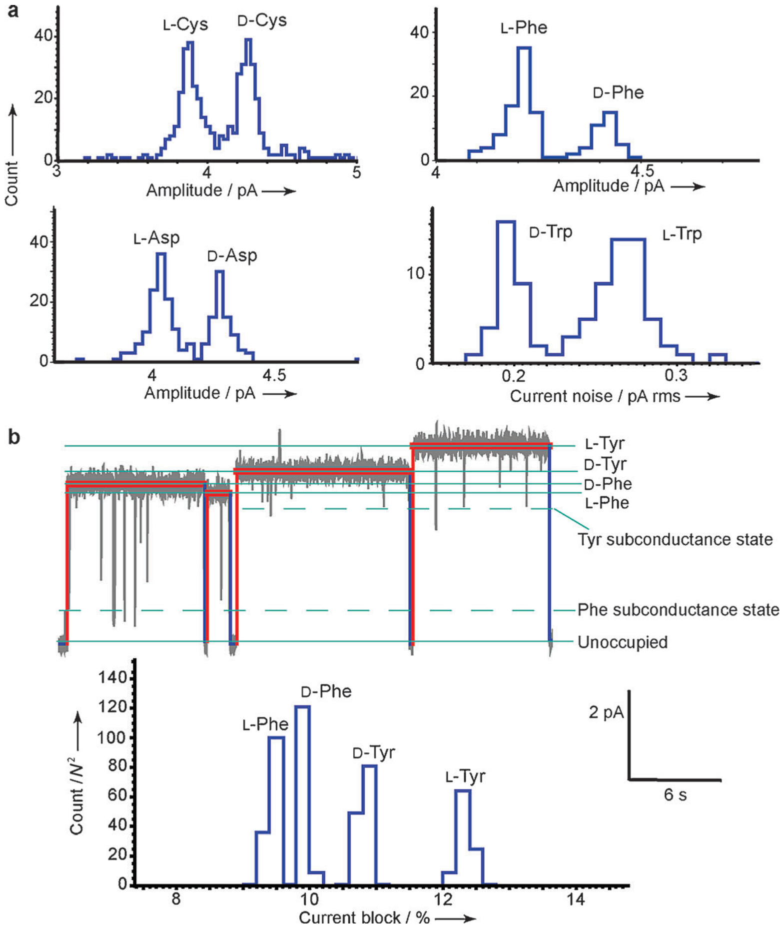

Figure 3. Detection of enantiomers in a mixture of amino acids. a) Event histograms of the current amplitudes of the blocking events observed in the presence of the enantiomers of cysteine (Cys), phenylalanine (Phe), and aspartic acid (Asp). In the case of tryptophan the rms current noise of the current blocks is displayed. For the corresponding current traces, see the Supporting Information. b) Representative current trace from a mixture of D,L-tyrosine and D,L-phenylalanine (1 µM of each enantiomer). See the Supporting Information for a longer trace. The red line corresponds to the idealized trace obtained from a single-channel search using Clampfit. The experimental conditions are the same as in Figure 2.

(0.27 ± 0.03 pA, $n = 52$ events) compared to D-tryptophan (0.20 ± 0.02 pA, $n = 32$ events). The difference in rms noise might be caused by a change in conformational freedom of the complex, resulting from interactions with neighboring amino acid residues in the lumen of the pore. The enantiomers of leucine and histidine could not be distinguished by using this Cu^{II}–phenanthroline nanopore (see the Supporting Information).

An additional challenge was to determine enantiomeric excess for multiple amino acids simultaneously. To achieve *ee* detection in a mixture, the amplitude of current block, the mean binding duration, and excess noise during the block were used to identify the amino acids (Figure 3b and the Supporting Information). As proof of principle, the four enantiomers of phenylalanine and tyrosine were examined (Figure 3b). The four molecules were clearly distinguished on the basis of current block by visual inspection of current traces and in an amplitude event histogram. Moreover, specific sub-conductance states within the current blockades could be used to separate phenylalanine and tyrosine; the blockades arising from phenylalanine contained short reversible steps to less blocked levels (0.5 ± 0.1 pA and 0.7 ± 0.3 pA, average lifetime 15 ± 1 ms, frequency of occurrence 0.6 ± 0.1 s^{-1}, $n = 92$ events), while the sub-conductance states during tyrosine blockades were of greater amplitude (2.3 ± 0.2 pA, average lifetime 4.1 ± 0.1 ms, frequency of occurrence 0.5 ± 0.1 s^{-1}, $n = 146$ events). These short events are likely to arise from different coordination modes of the amino acid with the copper(II) complex. Another example of an amino acid that induces a specific pattern of current block, allowing facile identification, is cysteine. Blockades due to cysteine were followed by additional steps to a lower current block in 39 ± 20 % ($n = 3$ pores) of the cases (see the Supporting Information). Possibly, cysteine switches to a different coordination geometry prior to dissociation. These results show that enantiomeric excess can be determined in mixtures of amino acids.

To demonstrate the continuous determination of *ee* in real time, we treated racemic tyrosine with L-tyrosine decarboxylase (Figure 4a), converting L-tyrosine to tyramine but leaving D-tyrosine intact. We found that the tyramine generated during this kinetic resolution did not bind copper(II). The addition of enzyme led to the disappearance of the current blockades corresponding to L-tyrosine (Figure 4b). The events corresponding to each enantiomer were logged in cumulative plots (Figure 4c). The plot of the D-tyrosine events is linear, as the concentration of D-tyrosine does not change with time. In the case of L-tyrosine, the cumulative plot fits well to an exponential function, as expected for a decay with a first-order dependence on L-tyrosine. Because the time-dependence of the derivative of a cumulative plot reflects the change in concentration of an analyte with time (see the Supporting Information), and the initial and final concentrations of L-tyrosine are known, the concentration of L-tyrosine during the enzymatic digestion can be calculated, and yields the variation of *ee* with time (Figure 4c).

In conclusion, we have developed a means to discriminate between the enantiomers of underivatized amino acids by stochastic sensing in real time with a Cu^{II}–phenanthroline protein nanopore. Rapid read-outs can be achieved, and the accuracy is increased by extended measurement times. The potential of the methodology has been demonstrated by the observation of the increase in the *ee* of tyrosine during an enzymatic kinetic resolution. Combined with ongoing improvements in bilayer technology, the approach will permit the screening of many reactions simultaneously in small volumes in parallel formats,[19–23] for example, to allow the simultaneous screening of numerous catalysts for enan-

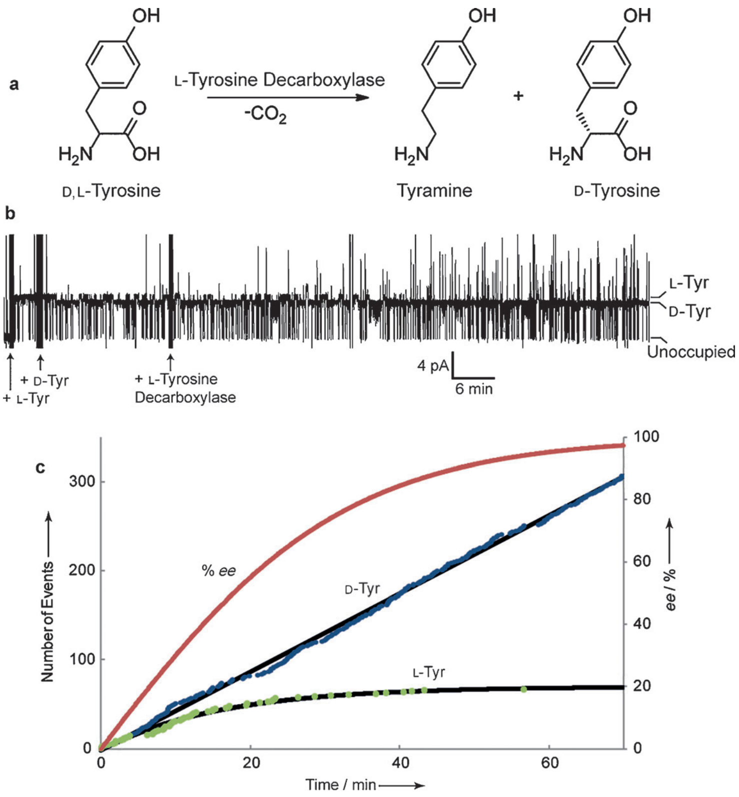

Figure 4. Treatment of D,L-tyrosine with L-tyrosine decarboxylase from *Streptococcus faecalis*. a) The reaction catalyzed by a cell extract containing the enzyme. L-Tyrosine is converted to tyramine, which does not bind copper(II), enriching the solution in D-tyrosine. b) Current recording during the digest. Conditions: 6 μM D,L-tyrosine and L-tyrosine decarboxylase (0.7 mg cell extract ml^{-1}) added from the *cis* compartment, 10 μM $CuCl_2$ added from the *trans* compartment, both in 1 M KCl, 10 mM MOPS, pH 7.0. The applied potential was −50 mV. At longer reaction times, spikes to a higher blocking level occur, which may originate from components of the cell extract. c) Cumulative plot of the reaction progress. The number of events that correspond to L-tyrosine decreases over time and the plot fits the exponential $N(t) = -225\exp(t/9.71\times10^{5}) + 69.8$, with N = accumulated number of events, t = reaction time (in minutes), and $R^2 = 0.99$. The curve denoted "% *ee*" represents the change in *ee* with time. The *ee* is calculated from the concentrations of D- and L-tyrosine, which are determined from the derivatives of the cumulative plots as described in the Supporting Information.

tioselectivity. The *ee* of several amino acids can be compared simultaneously in a mixture by using a single nanopore when different current characteristics allow for discrimination between the components. Furthermore, as illustrated in the reaction with a crude extract of L-tyrosine decarboxylase, contaminants either do not bind the copper in the pore, or the signals arising from the contaminants can be identified and ignored.

Received: July 17, 2012

Keywords: amino acids · biosensors · chirality · copper · membrane proteins

[1] *Quantitation of amino acids and amines by chromatography: methods and protocols* (Ed.: I. Molnár-Perl), Elsevier, Amsterdam, **2005**.
[2] A. Inamoto, K. Ogasawara, K. Omata, K. Kabuto, Y. Sasaki, *Org. Lett.* **2000**, *2*, 3543.
[3] G. Grigorean, J. Ramirez, S. H. Ahn, C. B. Lebrilla, *Anal. Chem.* **2000**, *72*, 4275.
[4] J. F. Folmer-Andersen, V. M. Lynch, E. V. Anslyn, *J. Am. Chem. Soc.* **2005**, *127*, 7986.
[5] X. Mei, C. Wolf, *J. Am. Chem. Soc.* **2006**, *128*, 13326.
[6] D. Leung, J. F. Folmer-Andersen, V. M. Lynch, E. V. Anslyn, *J. Am. Chem. Soc.* **2008**, *130*, 12318.
[7] H. Bayley, P. S. Cremer, *Nature* **2001**, *413*, 226.
[8] L.-Q. Gu, O. Braha, S. Conlan, S. Cheley, H. Bayley, *Nature* **1999**, *398*, 686.
[9] X.-f. Kang, S. Cheley, X. Guan, H. Bayley, *J. Am. Chem. Soc.* **2006**, *128*, 10684.
[10] C. Gao, S. Ding, Q. Tan, L.-Q. Gu, *Anal. Chem.* **2009**, *81*, 80.
[11] C. Han, X. Hou, H. Zhang, W. Guo, H. Li, L. Jiang, *J. Am. Chem. Soc.* **2011**, *133*, 7644.
[12] M. V. Rekharsky, Y. Inoue, *Chem. Rev.* **1998**, *98*, 1875.
[13] A. J. Boersma, K. L. Brain, H. Bayley, *ACS Nano* **2012**, DOI: 10.1021/nn301125y.
[14] L. Antolini, G. Marcotrigiano, L. Menabue, G. C. Pellacani, M. Saladini, M. Sola, *Inorg. Chem.* **1985**, *24*, 3621.
[15] H. Masuda, T. Sugimori, A. Odani, O. Yamauchi, *Inorg. Chim. Acta* **1991**, *180*, 73.
[16] T. Sugimori, K. Shibakawa, H. Masuda, A. Odani, O. Yamauchi, *Inorg. Chem.* **1993**, *32*, 4951.
[17] O. Yamauchi, A. Odani, *J. Am. Chem. Soc.* **1985**, *107*, 5938.
[18] T. Sugimori, H. Masuda, N. Ohata, K. Koiwai, A. Odani, O. Yamauchi, *Inorg. Chem.* **1997**, *36*, 576.
[19] R. Syeda, M. A. Holden, W. L. Hwang, H. Bayley, *J. Am. Chem. Soc.* **2008**, *130*, 15543.
[20] H. Bayley, B. Cronin, A. Heron, M. A. Holden, W. L. Hwang, R. Syeda, J. Thompson, M. Wallace, *Mol. Biosyst.* **2008**, *4*, 1191.
[21] A. J. Heron, J. R. Thompson, B. Cronin, H. Bayley, M. I. Wallace, *J. Am. Chem. Soc.* **2009**, *131*, 1652.
[22] T. Osaki, H. Suzuki, B. Le Pioufle, S. Takeuchi, *Anal. Chem.* **2009**, *81*, 9866.
[23] G. Baaken, N. Ankri, A. K. Schuler, J. Ruhe, J. C. Behrends, *ACS Nano* **2011**, *5*, 8080.